Separation Science and Technology
Publication details, including instructions for authors and subscription information:
http://www.informaworld.com/smpp/title~content=t713708471

A Study of Concentration Polarization Phenomenon on the Surface of a Gas Separation Membrane

K. Haraya[a]; T. Hakuta[a]; H. Yoshitome[a]; S. Kimura[b]
[a] NATIONAL CHEMICAL LABORATORY FOR INDUSTRY YATABE, TSUKUBA, IBARAKI, JAPAN [b] INSTITUTE OF INDUSTRIAL SCIENCE UNIVERSITY OF TOKYO, TOKYO, JAPAN

To cite this Article Haraya, K. , Hakuta, T. , Yoshitome, H. and Kimura, S.(1987) 'A Study of Concentration Polarization Phenomenon on the Surface of a Gas Separation Membrane', Separation Science and Technology, 22: 5, 1425 — 1438
To link to this Article: DOI: 10.1080/01496398708058408
URL: http://dx.doi.org/10.1080/01496398708058408

SEPARATION SCIENCE AND TECHNOLOGY, **22**(5), pp. 1425-1438, 1987

A Study of Concentration Polarization Phenomenon on the Surface of a Gas Separation Membrane

K. HARAYA, T. HAKUTA, and H. YOSHITOME

NATIONAL CHEMICAL LABORATORY FOR INDUSTRY
YATABE, TSUKUBA, IBARAKI 305 JAPAN

S. KIMURA

INSTITUTE OF INDUSTRIAL SCIENCE
UNIVERSITY OF TOKYO
TOKYO 106 JAPAN

Abstract

Mass transfer coefficients on the surface of porous glass membrane were obtained from separation tests of H_2-CO mixtures. These data agree with the correlation presented by Ghosh and Upadhyay for mass transfer on an impermeable wall. In addition, effects of the selectivity of membrane and bulk composition on the concentration polarization phenomenon are discussed and the limiting permeability which is affected by the polarization is represented as a function of mass transfer coefficient.

INTRODUCTION

It is well known that the concentration boundary layer always exists on a membrane surface and decreases the efficiency in separation processes, such as electrodialysis, reverse osmosis, and ultrafiltration. In the concentration boundary layer, a faster permeating component decreases and a slower permeating component increases in the direction normal to the membrane surface, resulting in the concentration polarization phenomenon between the bulk fluid and the membrane surface. If diffusive fluxes of components due to concentration gradients are much greater than the permeation flux of fluid, the concentration polarization phenomenon becomes negligible small.

Although a large number of studies on gas separation with membranes have been reported, there have been only a few papers (*1*, *2*) which examine the concentration polarization phenomenon. Investigators could ignore the polarization effect since most of membranes used in that work had too low permeabilities to form the concentration boundary layer. Recently, permeabilities of gas separation membranes have becoming important due to the advance of membrane fabrication technology. We must know how the mass transfer rate on the surface of a gas separation membrane and the limiting permeability which is affected by the concentration polarization can be expressed.

This paper presents results of experiment using a porous glass membrane of a capillary tube which has a sufficiently large flux to investigate the concentration polarization. In addition, general relations which control the polarization are discussed.

FUNDAMENTAL EQUATIONS

Gas species of A and B are conveyed by permeation flux to the membrane surface, and a Component A permeates faster than B, resulting in a decrease of the fraction of A in the direction normal to the membrane surface as illustrated in Fig. 1. Then, the mass balance of Component A on a cylindrical differential element within the boundary layer is given as

$$rN_A = rx(N_A + N_B) + rCD\frac{dx}{dr} \tag{1}$$

Using the relation $y = N_A/(N_A + N_B)$, the following equation is derived at steady state:

$$\frac{d}{dr}\left\{r\frac{CD}{1-(x/y)}\frac{dx}{dr}\right\} = 0 \tag{2}$$

Boundary conditions are

$$\begin{aligned} x &= x_m \quad \text{at} \quad r = r_m \\ x &= x_b \quad \text{at} \quad r = r_b \end{aligned} \tag{3}$$

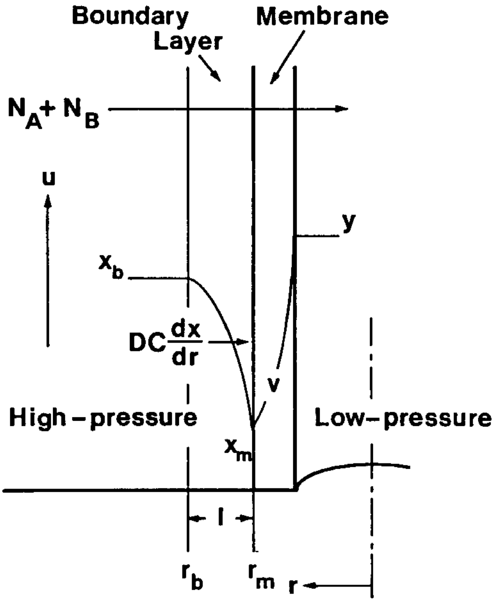

FIG. 1. Schematic representation of concentration polarization.

Integration of Eq. (2) gives the following concentration profile:

$$\frac{y - x}{y - x_b} = \left(\frac{y - x_m}{y - x_b}\right)^{\frac{\ln (r/r_b)}{\ln (r_m/r_b)}} \tag{4}$$

From Eq. (4), the product of radius and total permeation flux can be obtained as

$$r_m(N_{A,m} + N_{B,m}) = -k \cdot C \cdot r_{av} \cdot \ln M \tag{5}$$

where

$$k = D/l \tag{6}$$

$$r_{av} = l/\ln (r_b/r_m) \tag{7}$$

$$M = \frac{y - x_b}{y - x_m} \tag{8}$$

k is a mass transfer coefficient, r_{av} is a logarithmic mean radius of the concentration boundary layer, and M is a modulus of the concentration polarization. Using a volume flux, modification of Eq. (5) yields

$$M = \exp(-J_v/k) \tag{9}$$

where

$$J_v = \frac{(N_{A,m} + N_{B,m})r_m}{C \cdot r_{av}} \tag{10}$$

J_v is the volume flux of the total permeate based on a logarithmic mean area of the concentration boundary layer.

One can determine k by substituting M and J_v into Eq. (9). In the separation test of a binary mixture with membrane, the values of x_b and y are obtainable directly from the experiment, and J_v is also obtainable from Eq. (10) when r_{av} is a known value. Then x_m can be estimated by the permeation rate equation. In this work, r_m/r_{av} was assumed to equal 1, and x_m was estimated by the permeation equation of Present and de Bethune (*3*) (see Appendix).

EXPERIMENTAL

A porous glass membrane was supplied by Toyobo Co., Ltd. The shape of the membrane was a capillary tube of 1.9 mm o.d. and 1 mm i.d., and 10 nm of the average pore radius was determined from mercury porosimetry. A schematic diagram of the experimental apparatus is illustrated in Fig. 2. The capillary membrane was fixed to the metal plug tube by epoxy resin and fitted in the permeation cell. The membrane area of permeable section was controlled by a coating of epoxy resin on the part of the capillary near the metal plug. The permeable section was placed at a point apart from the gas inlet and outlet to eliminate the influence of disturbance of velocity.

Separation tests were carried out with H_2-CO mixtures at 373 K. Flow rate ratios of permeate to feed were maintained below 0.01 to avoid the effect of flow pattern on the separation efficiency. Operating pressures of feed and nonpermeate stream were about 1.1 MPa, and those of permeate stream were changed from 0.2 to 0.6 MPa to vary the permeation flux. Gas flow rate was measured by a soap-film flowmeter and the composition was analyzed by gas chromatography. The ranges of various parameters covered in the present work are given in Table 1.

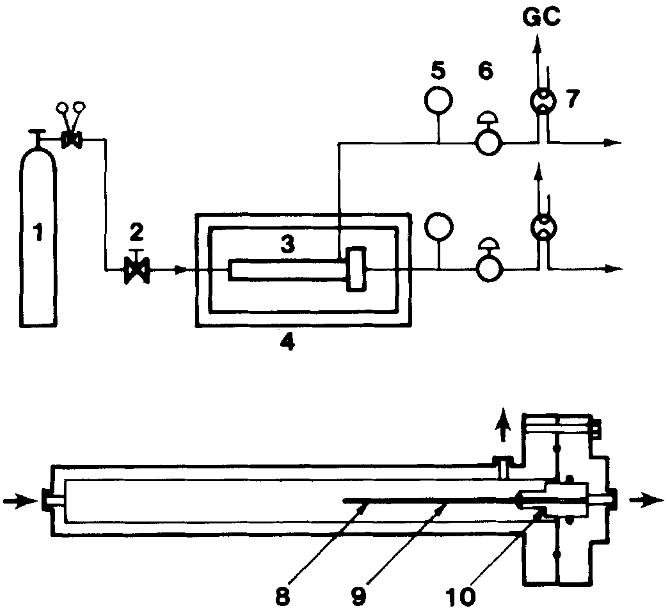

FIG. 2. Schematic diagram of experimental apparatus. 1: Cylinder of mixed gas. 2: Flow control valve. 3: Permeation cell. 4: Heater. 5: Pressure gauge. 6: Pressure regulator. 7: Sampling valve. 8: Membrane (permeable section). 9: Membrane (impermeable section). 10: Metal plug.

TABLE 1
Range of Operating Variables

K_{O,H_2} (nmol · m · s^{-1} · m^{-2} · Pa^{-1})	2.4
$K_{O,H_2}/K_{O,CO}$	3.74
d_o (cm)	0.7-1.92
d_i (cm)	0.19
L (cm)	0.45-0.96
a	0.099-0.271
d_e/L	0.531-3.84
P_h (MPa)	1.1
p_l (MPa)	0.1-0.6
D (cm^2/s)	0.106 at 1.1 MPa
η/ρ (cm^2/s)	0.025-0.047 at 1.1 MPa
Re	110-560
Sc	0.24-0.44

RESULTS AND DISCUSSION

In this work, H_2-CO mixtures are considered as ideal gases whose viscosities and diffusivities were evaluated by Wilke's (*4*) equation and the correlation of Marrero and Mason (*5*), respectively.

The M values obtained here were always lower than 1. The experimental results in the case of the length of membrane, L, was 0.96 cm and equivalent diameters of the permeation cell, d_e, were 0.5–1.73 cm (shown in Fig. 3), where M is plotted against J_v with the product of Reynolds and Schmidt numbers as a parameter. M decreases with an increase of J_v and a decrease of Re · Sc. Figure 4 shows the experimental results in the case of $L = 0.45$ cm and $d_e = 1.73$ cm as a plot of M vs $1/u$ with J_v as a parameter. M decreases with increases of $1/u$ and J_v.

From the tendency of the experimental results, a decrease of M is interpreted as due to concentration polarization. Using these data, mass transfer coefficients were calculated by Eq. (9) and the results are shown in Fig. 5 as a Sh vs $\mathrm{Re} \cdot \mathrm{Sc}(d_e/L)\Phi(a)$ plot. The solid line in the figure is obtained from

$$\mathrm{Sh} = 2.703[\mathrm{Re} \cdot \mathrm{Sc}(d_e/L)\Phi(a)]^{0.33} \qquad (11)$$

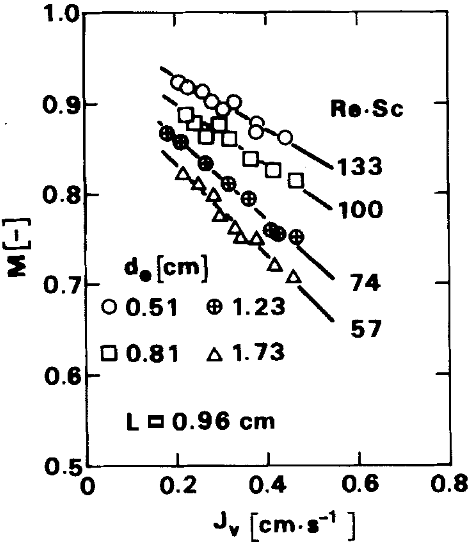

FIG. 3. Effect of permeation flux on the modulus of concentration polarization.

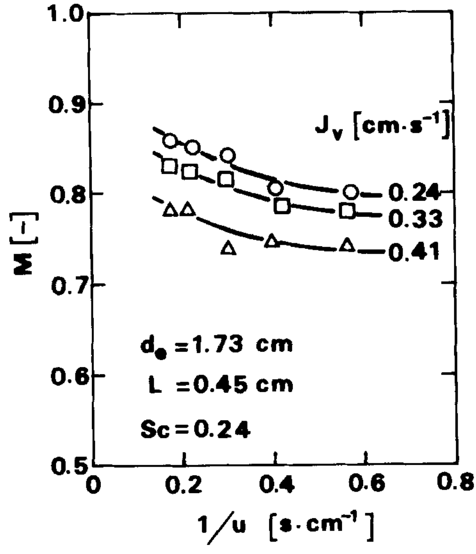

FIG. 4. Effect of flow velocity on the modulus of concentration polarization.

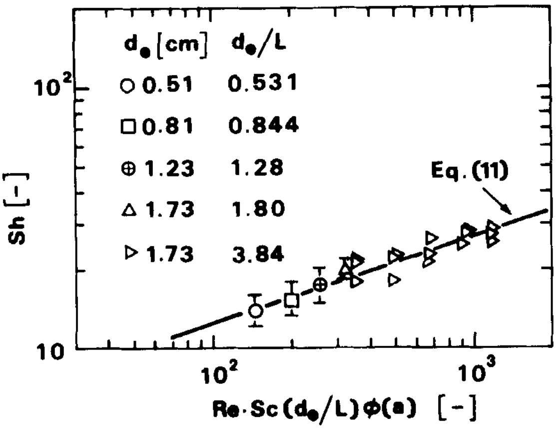

FIG. 5. Comparisons of mass transfer coefficient between experimental and calculated values by Ghosh and Upadhyay correlation.

where

$$\Phi(a) = \frac{1-a}{a}\left[\frac{0.5 - \dfrac{a^2}{(1-a^2)}\ln(1/a)}{\dfrac{(1+a^2)}{(1-a^2)}\ln(1/a) - 1}\right] \tag{12}$$

Equation (11) was given by Ghosh and Upadhyay (*6*) for the mass transfer on a short annular impermeable wall with developing concentration and hydrodynamic boundary layers in the laminar regime. The experimental results obtained from the porous membrane agree fairly well with Eq. (11) (average deviation ±20%).

The values of k obtained here range from about 1 to 3 cm/s and the evaluated thicknesses of the boundary layers range from about 0.3 to 1 mm. Due to the assumption of $r_m/r_{av} = 1$, evaluated k may be 20–30% larger than true values, but is probably within experimental errors.

Discussion on the Limiting Permeability Which Is Affected by the Concentration Polarization

Gas separation membranes investigated or used commercially range in selectivity from 2 (O_2/N_2 separation) to more than 100 (He/CH_4 separation). In the following, the effects of the selectivity of membrane and bulk composition on the concentration polarization phenomena are discussed, and the limiting permeation rates which are affected by the polarization are represented.

For simplicity, assume that the permeability of each component is independent of partial pressure. Permeation fluxes of component gases are given as

$$N_A = Q_A p_h (x_m - Pry) \tag{13}$$

$$N_B = Q_B p_h \{(1 - x_m) - Pr(1 - y)\} \tag{14}$$

where $Pr = p_l/p_h$. From Eqs. (13) and (14) the relation between x_m and y is given as

$$\frac{y}{1-y} = \alpha_0 \frac{x_m - Pry}{1 - x_m - Pr(1-y)} \tag{15}$$

and J_v is given as

$$J_\omega = \frac{Q_A p_h}{C}\left[x_m - Pry + \frac{1}{\alpha_0}\{(1 - x_m) - Pr(1 - y)\}\right] \qquad (16)$$

where $\alpha_0 = Q_A/Q_B$, which is sometimes called the ideal separation factor.

The calculation procedures to obtain the relation between M and permeability are as follows: (1) Assume x_m and calculate y by Eq. (15) under arbitrary fixed conditions of x_b, α_0, Pr, k, and M. Repeat this procedure until the value of $(y - x_b)/(y - x_m)$ becomes equal to M. (2) Calculate J_ω by Eq. (9) and then calculate $Q_A p_h/C$ by Eq. (16).

The meaning of $Q_A p_h/C$ is a volume flux of pure Component A at the operating temperature T and pressure p_h. The volume permeation rate Q'_A at the standard T_0 and p_0 are given as

$$Q'_A = \frac{Q_A p_h}{C}\frac{T_0}{p_0 T} \qquad (17)$$

The effects of α_0 and x_b on the relation between M and $Q_A p_h/C$ at $Pr = 0$ are shown in Figs. 6 and 7, respectively. When a k and a membrane permeability are constant, lower α_0 and higher x_b bring about a large decrease of M because of large flux of the total permeate. The limiting permeation fluxes, which are defined by $Q_A p_h/C$ corresponding to

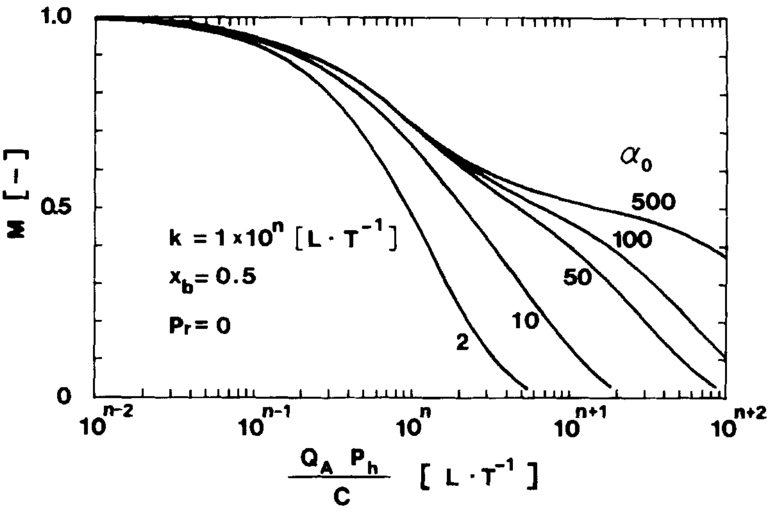

FIG. 6. Effect of membrane selectivity on the modulus of concentration polarization.

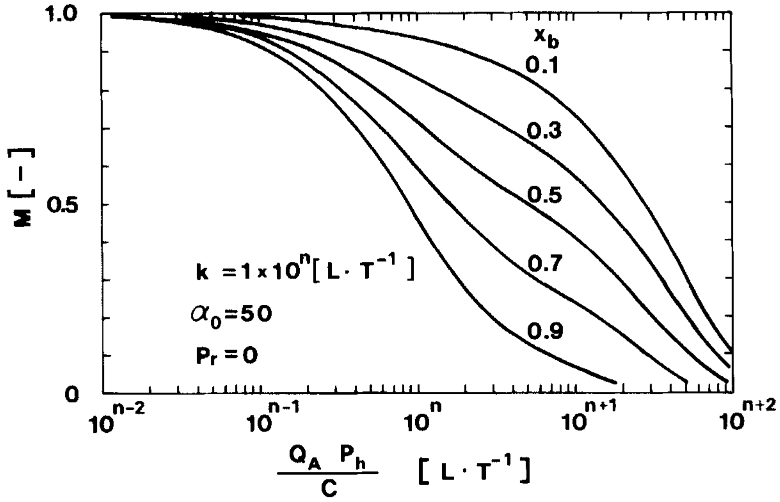

FIG. 7. Effect of bulk composition on the modulus of concentration polarization.

$M = 0.95$ in this study, are illustrated as a function of k in Fig. 8. From this figure, one can estimate the limiting permeation rate which is affected by the concentration polarization phenomenon. For example, when air of 100 $cm^3(STP) \cdot s^{-1}$ is fed into the annular tube module in which $d_i = 5$ mm, $d_o = 10$ mm, and $L = 2$ m, the calculated k by Eq. (11) is 1.2 cm/s. In this case the limiting permeation rate, Q'_A, is estimated approximately as 1×10^{-3} $cm^3(STP) \cdot s^{-1} \cdot cm^{-2} \cdot cmHg^{-1}$ ($\alpha_0 = 2$, $p_h = 76$ cmHg, $Pr = 0$). This value is the same level as the O_2 permeation rate of 1000 Å thick P-11 membrane (*7*) and is one order in magnitude smaller than those of 500 Å thick polydimethyl silicone composite (*8*) and of 1000 Å thick polyacetylenes (*9*). It is suggested that the concentration polarization phenomenon is an important problem in the development of an oxygen enrichment permeator.

CONCLUSIONS

1. The mass transfer coefficient measured on the surface of a porous glass membrane agreed with the correlation for the mass transfer on an impermeable wall.
2. By an analytical study, effects of the selectivity of membrane and bulk composition on the concentration polarization phenomenon were

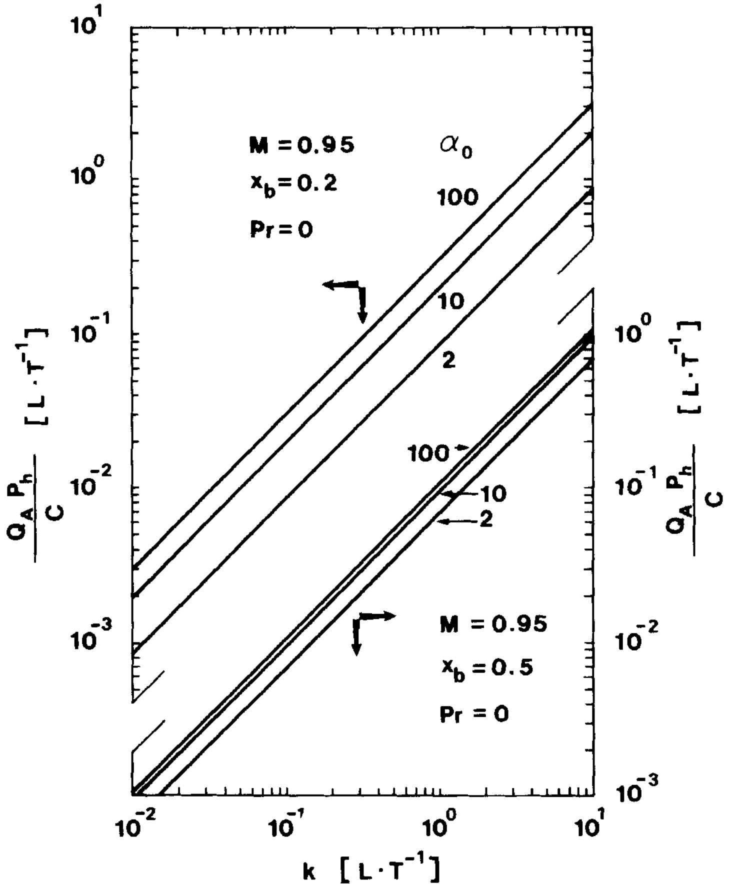

FIG. 8. Relations between mass transfer coefficient and limiting permeation flux which is affected by the concentration polarization (M = 0.95).

made clear and the limiting permeability which is affected by the polarization was represented as a function of the mass transfer coefficient.

APPENDIX

Applying the capillary model presented by Present and deBethune (*3*), the permeation flux of each component of an A–B binary mixture can be written as follows using observed Knudsen permeabilities based on a logarithmic mean area (*2*):

$$N_A = -K_{O,A}\left\{\frac{1}{1+bp}\frac{d\upsilon p}{dr} + \frac{f_A bp}{1+bp}\upsilon\frac{dp}{dr} + \upsilon a_A p\frac{dp}{dr}\right\} \quad \text{(A-1)}$$

$$N_B = -K_{O,B}\left\{\frac{1}{1+bp}\frac{d(1-\upsilon)p}{dr} + \frac{f_B bp}{1+bp}(1-\upsilon)\frac{dp}{dr} + (1-\upsilon)a_B p\frac{dp}{dr}\right\} \quad \text{(A-2)}$$

where

$$a_A = 3r_p/(16\eta V_A), \qquad a_B = 3r_p/(16\eta V_B) \quad \text{(A-3)}$$

$$b = \frac{8r_p}{3\pi}\sqrt{\frac{\pi kT}{2m_A m_B}}\,\frac{\upsilon\sqrt{m_A} + (1-\upsilon)\sqrt{m_B}}{pD} \quad \text{(A-4)}$$

$$f_A = \frac{\sqrt{m_A}}{\upsilon\sqrt{m_A} + (1-\upsilon)\sqrt{m_B}}, \qquad f_B = \frac{\sqrt{m_B}}{\upsilon\sqrt{m_A} + (1-\upsilon)\sqrt{m_B}} \quad \text{(A-5)}$$

The composition ratio of the permeates can be given by

$$\frac{y}{1-y} = \frac{N_A}{N_B} \quad \text{(A-6)}$$

Combination of Eqs. (A-1), (A-2), and (A-6) gives

$$\frac{d\upsilon}{dp} = \frac{1}{p\{\alpha_0(1-y)+y\}}[\alpha_0\upsilon(y-1)\{f_A bp + a_A p(1+bp) + 1\} + y(1-\upsilon)\{f_B bp + a_B p(1+bp) + 1\}] \quad \text{(A-7)}$$

x_m is obtainable by integrating Eq. (A-7) from $\upsilon = y$ at $p = p_l$ to $p = p_h$, taking into account the change of viscosity along the membrane thickness. Experimental and calculated values by Eq. (A-7) are in good agreement when the concentration polarization is negligibly small (*2*).

SYMBOLS

a	aspect ratio defined by d_i/d_o
a_A, a_B	parameters defined by Eq. (A-3) $((M \cdot L^{-1} \cdot T^{-2})^{-1})$
b	parameter defined by Eq. (A-4) $((M \cdot L^{-1} \cdot T^{-2})^{-1})$
C	total molar concentration $(mol \cdot L^{-3})$
D	mutual diffusion coefficient $(L^2 \cdot T^{-1})$
d_e	equivalent diameter, $d_o - d_i$ (L)
d_i	outer diameter of membrane, i.e., inner tube (L)
d_o	diameter of permeation cell, i.e., outer tube (L)
f_A, f_B	parameters defined by Eq. (A-5)
J_v	total volume flux defined by Eq. (10) $(L^3 \cdot L^{-2} \cdot T^{-1})$
K_O	Knudsen permeability $(mol \cdot L \cdot L^{-2} \cdot T^{-1} \cdot (M \cdot L^{-1} \cdot T^{-2})^{-1})$
k	mass transfer coefficient defined by Eq. (6) $(L \cdot T^{-1})$ and Boltzmann constant in Eq. (A-4) $(J.K^{-1})$
L	length of permeable section (L)
l	thickness of concentration boundary layer (L)
N	molar flux $(mol \cdot L^{-2} \cdot T^{-1})$
M	modulus of concentration polarization defined by Eq. (8)
m	weight of a gas molecule (M)
p	total pressure $(M \cdot L^{-1} \cdot T^{-2})$
Pr	pressure ratio defined by p_l/p_h
Q	molar permeation rate $(mol \cdot L^{-2} \cdot T^{-1} \cdot (M \cdot L^{-1} \cdot T^{-2})^{-1})$
Q'	volume permeation rate $(L^3(STP) \cdot L^{-2} \cdot T^{-1} \cdot (M \cdot L^{-1} \cdot T^{-2})^{-1})$
Re	Reynolds number, $d_e u \rho/\eta$
r	radial distance in cylindrical coordinate (L)
r_{av}	logarithmic mean radius of concentration boundary layer (L)
r_p	pore radius of porous membrane (L)
Sc	Schmidt number, $\eta/\rho D$
Sh	Sherwood number, kd_e/D
T	absolute temperature (K)
u	average flow velocity of bulk fluid $(L \cdot T^{-1})$
V	average velocity of gas molecule $(L.T^{-1})$
v	mole fraction of A in membrane
x	mole fraction of A on high-pressure stream
y	mole fraction of A on low-pressure stream

Greek

α_0	ideal separation factor defined by Q_A/Q_B or $K_{O,A}/K_{O,B}$
η	viscosity of gas $(M \cdot L^{-1}T^{-1})$
ρ	density of gas $(M \cdot L^{-3})$

Subscripts

A	faster permeating component
B	slower permeating component
b	bulk fluid
h	high-pressure stream
l	low-pressure stream
m	membrane surface
O	standard temperature and pressure

Acknowledgment

This work is a part of the results of "C_1 Chemistry Project," a National Research and Development Program of the Agency of Industrial Science and Technology, Ministry of International Trade and Industry (M.I.T.I.), Japan.

REFERENCES

1. Y. Suzuki and S. Kimura, *J. At. Energy Soc. Jpn., 26,* 802 (1984).
2. K. Haraya, Y. Shindo, T. Hakuta, and H. Yoshitome, *J. Chem. Eng. Jpn., 19,* 186 (1986).
3. R. D. Present and A. J. deBethune, *Phys. Rev., 75,* 1050 (1949).
4. C. R. Wilke, *J. Chem. Phys., 18,* 517 (1950).
5. T. R. Marrero and E. A. Mason, *J. Phys. Chem. Ref. Data, 1,* 3 (1972).
6. U. K. Ghosh and S. N. Upadhyay, *AIChE J., 31,* 1721 (1985).
7. W. J. Ward, W. R. Browall, and R. M. Salemme, *J. Membr. Sci., 1,* 59 (1976).
8. R. L. Riley and R. L. Grabowsky, U.S. Patent 4,243,701 (1981).
9. K. Takada, H. Matsuya, T. Masuda, and T. Higashimura, *J. Appl. Polym. Sci., 30,* 1605 (1985).

Received by editor August 25, 1986